NATIONAL ADVISORY COMMITTEE FOR AERONAUTICS

TECHNICAL NOTE

No. 1734

INVESTIGATION OF THE VARIATION OF MAXIMUM LIFT FOR A PITCHING AIRPLANE MODEL AND COMPARISON WITH FLIGHT RESULTS

By Paul W. Harper and Roy E. Flanigan

Langley Aeronautical Laboratory
Langley Field, Va.

Washington
October 1948

NATIONAL ADVISORY COMMITTEE FOR AERONAUTICS

TECHNICAL NOTE NO. 1734

INVESTIGATION OF THE VARIATION OF MAXIMUM LIFT FOR A PITCHING AIRPLANE MODEL AND COMPARISON WITH FLIGHT RESULTS

By Paul W. Harper and Roy E. Flanigan

SUMMARY

Apparatus was developed which utilized a pitching airplane model to determine maximum wing loads as a function of the rate of change of angle of attack. In order to evaluate the pitching-model technique, maximum lift coefficients were determined in wind-tunnel investigations of a $\frac{1}{20}$-scale model of a conventional single-engine fighter airplane and were compared with existing flight data for this airplane. The wind-tunnel investigation extended through a Mach number range from approximately 0.2 to 0.6 at pitching velocities comparable to flight values obtained with the test airplane in abrupt pull-ups. The wind-tunnel and flight results were found to be in good agreement.

INTRODUCTION

Although variations of maximum lift with pitching velocity were observed as early as 1930, only very limited quantitative information concerning the phenomenon has been obtained notwithstanding its importance in relation to the high-speed aircraft of recent years. Previous wind-tunnel investigations of this effect have been made only at low Mach numbers and have been concerned primarily with constant section airfoils; flight investigations have not been planned specifically to provide systematic data of this nature.

The need for more complete information concerning the dependence of maximum wing loads on pitching velocity as a function of various parameters thus prompted the development of an experimental technique which utilized an airplane model capable of being pitched at various rates through maximum lift. Such a device would not involve the hazards of flight testing in the stall region at high speeds and would make possible a systematic study of the separate effects of the variables involved because the various parameters could be more easily controlled.

The use of small models made it necessary to establish the applicability of pitching model results in the prediction of full-scale flight loads. For this purpose the maximum lift coefficients were determined in the Langley 7- by 10-foot high-speed tunnel as functions of the rate of change of angle of attack for a model of the test airplane for which maximum lift coefficients obtained in flight were presented in reference 1. The results are given herein and are compared with flight data obtained on the test airplane. The tunnel and flight tests were made over a corresponding Mach number range from approximately 0.2 to 0.6 and an equivalent pitching-velocity range.

SYMBOLS

c	chord length, feet
C_L	lift coefficient
$C_{L_{max}}$	maximum lift coefficient
$\Delta C_{L_{max}}$	difference between corresponding maximum lift coefficients of airplane and model
M	Mach number
q	dynamic pressure, pounds per square foot
R	Reynolds number
S	wing area, square feet
V	true airspeed, feet per second
W	airplane weight, pounds
α	angle of attack, degrees
$d\alpha/dt$	rate of change of angle of attack, radians per second
$(d\alpha/dt)_e$	$d\alpha/dt$ of model equivalent to test-airplane values, radians per second
$dC_L/d\alpha$	slope of lift curve, per radian
dn/dt	rate of change of airplane normal load factor with time

APPARATUS

The model and its pitching mechanism were mounted at opposite ends of a $6\frac{1}{2}$-foot, 3-inch-diameter, tubular steel boom as shown in the diagrammatic sketch of figure 1. The model was a $\frac{1}{20}$-scale partial reproduction of the test airplane and consisted of the wings and a truncated, propellerless fuselage. The 2-foot-span wing had an area of 3/4 square foot and a mean aerodynamic chord of 0.364 foot. As shown in figure 1, the wings and fuselage were mounted on a ball-bearing housing which rotated on a shaft through the end of a small cantilever beam. The rotating parts were statically balanced about the axis of rotation which was at 23 percent of the mean aerodynamic chord.

The pitching mechanism contained a variable-speed motor driving a cam with a spring-loaded follower which actuated the model through a cable-pulley system. Each cam revolution provided one complete pitching oscillation of the model and a dwell period between oscillations during which the model was held at a small negative angle of attack. The dwell period, which was equivalent to 50 chord lengths of travel at low test Mach numbers, permitted ample time for the aerodynamic flow to stabilize prior to each pull-up. The pitching velocity of the model during the pull-up was controlled by varying the cam speed. An operating speed of the cam which gave the model a pull-up velocity of 12 radians per second produced two complete oscillations of the model each second. The cam characteristics were such that the model accelerated from a small negative angle to a small positive angle while it acquired a given pitching velocity which was then maintained constant beyond the angle of maximum lift.

Devices were incorporated within the model for obtaining time histories of lift and angle of attack when used in conjunction with a multichannel recording oscillograph. Static lift forces could be determined to within 2 percent by the use of strain gages mounted on a beam designated in figure 1 as the lift beam. Errors in lift measurements arising from vibration of the lift-beam-model system were negligible because of the high natural frequency of the lift beam relative to the applied pitching frequency. (The natural frequency of the lift beam was approximately twenty times the maximum applied pitching frequency.) Pseudolift errors caused by dynamic unbalance coupled with angular acceleration of the rotating parts were found experimentally to be negligible. The variation of angle of attack with time was obtained by means of a cam-deflected strain-gage-equipped cantilever beam from which the rate of change of the angle of attack with time could be determined within 2 percent by graphical differentiation.

A photograph of the model and its pitching mechanism mounted in the Langley 7- by 10-foot high-speed tunnel is shown as figure 2. The pitching mechanism and the base of the boom were bolted to the tunnel vertical

mounting strut and covered with a steel fairing. The boom was supported 18 inches behind the model with four flexible steel cables preloaded to a value greater than the maximum expected lift forces of the model. A conservative estimate for the error in lift due to acceleration effects, based on computations involving the flexibility of this supporting system and the expected rate of application of lift forces, ranged from 2 to 5 percent.

WIND-TUNNEL INVESTIGATIONS

Scope

Time-history measurements were made of the lift and the angle of attack of the model at seven Mach number increments from 0.197 to 0.612 for pitching velocities $d\alpha/dt$ varying from approximately 3 to 12 radians per second. The relation of tunnel Reynolds number to Mach number is given in figure 3 which shows that the Reynolds number increased from 0.198×10^6 to 1.172×10^6 while the Mach number varied from 0.080 to 0.612.

Reduction of Data

A scale reproduction of a typical test record of lift and angle of attack recorded on the multichannel oscillograph is shown in figure 4. The particular record shown was taken at a tunnel free-stream Mach number of 0.400 where the pitching velocity of the model during the pull-up was 5.75 radians per second.

The character of the vibrations induced as the lift suddenly dropped from its maximum value may be seen in figure 4. Although the vibratory frequency of 39.2 cycles per second shown in this record tended to diminish slightly with Mach number, it was essentially constant for all tests and equal to the natural frequency of the model supporting system. Since the model vibrated predominantly at the natural frequency of the supporting system after stalling occurred, only the part of the record through maximum lift was used in evaluating results.

Typical time histories of lift coefficient and angle of attack of the model are presented in figure 5 for two Mach numbers and three pitching rates. In the reduction from the original records no corrections were made to the lift forces for either acceleration or wind-tunnel effects since these had been estimated to be small.

A nonlinear variation of the angle of attack with time was evident in some records as is shown in the three representative time variations of the angle of attack in figure 5. The variation given in figure 5(c) most nearly approaches the ideal in which the angle of attack increases linearly

with time up to maximum lift. The deviations from linearity, which were caused by the aerodynamic and inertia moments coupled with the elasticity of the control cables, made it necessary to establish a uniform method for finding $d\alpha/dt$ that would be applicable to the measured value of maximum lift coefficient. Several methods were considered for determining the effective values of $d\alpha/dt$ to be used in analyzing the data, such as the method in which $C_{L_{max}}$ was correlated with a slope at a number of chord lengths ahead of the point of $C_{L_{max}}$. A method was finally adopted in which the applicable $d\alpha/dt$ was taken as the slope of the line joining the point on the angular time history corresponding to zero lift with the point corresponding to maximum lift. The method was rationalized on the basis of an hypothesis, which has been frequently proposed, that the increase in lift is associated with the lag of flow separation brought about by the lag in the rate of growth of the boundary layer with angle of attack. The average slope, as obtained in the method adopted, thus gave an integrated effect of this slowed rate of growth.

Although the typical curves of C_L and α plotted against time given in figure 5 showed nonlinear variations, faired cross plots of C_L against α for the various pitching rates gave such typical variations as are shown in figure 6.

Results and Discussion

The main results of the wind-tunnel tests for the pitching model are presented in figure 7, in which the variation of maximum lift coefficient with rate of change of angle of attack is shown for each of the test Mach numbers. Straight lines, based on the least-squares method, have been faired through the test points for each Mach number.

Both the manner and rate of increase of $C_{L_{max}}$ with $d\alpha/dt$ are seen to vary with Mach number. Increments in $C_{L_{max}}$ can be noted which are as much as 50 percent above the static values obtained by extrapolation of the results to zero pitching velocity. The variation of $C_{L_{max}}$ with $d\alpha/dt$ is essentially linear at the higher Mach numbers, with no indication that any limit of increase had been reached. At the low Mach numbers, however, a leveling-off tendency exists which indicates that some limit of increase may have been reached. This leveling-off tendency is somewhat obscured by the scatter in the data and lack of sufficiently high values of $d\alpha/dt$. In view of the scatter and of the general character of the variations shown, a linear representation of all the data is believed justified.

The average deviation of the test points from values defined by the least-squares lines varies from $1\frac{1}{2}$ percent to $3\frac{1}{2}$ percent at different Mach numbers. These values represent larger individual point scatter than can be attributed to instrumental and estimated acceleration errors, which fact leads to the belief that actual variations in lift contribute to the scatter. These variations are considered to be due to nonuniformity of test conditions from point to point, such as dissimilarities in angle-of-attack time histories and variation in smoothness of the air flow due to vibration and kindred sources. The greatest amount of scatter occurring in the range of Mach numbers near 0.3 may be associated with the fact that in this range, according to reference 3, a transition from predominant Reynolds number effects to predominant Mach number effects on $C_{L_{max}}$ occurs.

TREATMENT OF FLIGHT DATA

The flight-test values of $C_{L_{max}}$ for the test airplane reported in reference 1 are presented in figure 8 as the square test symbols. These points are as originally presented and include a correction for tail load; thus, the flight lift coefficients are for a wing-fuselage configuration similar to that for the model.

Inasmuch as the angular velocities were not given in reference 1, some reworking of the original flight data was required in order to determine the pitching velocity $d\alpha/dt$ for each test point. The value of $d\alpha/dt$ during each pull-up was obtained from the original normal-acceleration and airspeed time-history records and from the equation

$$\frac{d\alpha}{dt} = \frac{W/S}{q} \frac{dn/dt}{dC_L/d\alpha}$$

The slope of the airplane normal load factor against time was taken as the slope of the line joining the points on the curve which correspond to unit load factor and maximum load factor. This method of determining dn/dt was comparable to that used for finding $d\alpha/dt$ of the pitching model.

The slope of the lift curve at the various Mach numbers was obtained from wind-tunnel tests of the propellerless 0.3-scale model of the test airplane reported in reference 2. Owing to a lack of information on the power conditions during the flight tests, power effects on $dC_L/d\alpha$ were neglected.

The airplane pitching velocity computed for each flight test point is listed in table I, along with the corresponding values of Mach number, maximum lift coefficient, and Reynolds number.

The wind-tunnel and flight values of $C_{L_{max}}$ should be compared on the basis of a common parameter which satisfies the condition for dynamic similitude. This condition requires that the unit rate of change of angle of attack per chord length of travel be equal for all quantities compared. The expression for the parameter satisfying this condition is $\frac{d\alpha}{dt}\frac{c}{V}$. Values of $d\alpha/dt$ equivalent to those for the test airplane were computed for the model by using this parameter and are listed in table I as $(d\alpha/dt)_e$.

The test points obtained in flight were insufficient to establish directly the relation of $C_{L_{max}}$ to $d\alpha/dt$ at the various Mach numbers. The relatively large number of test points in the Mach number region near 0.4, however, permitted the use of a graphical interpolation process which yielded values of $C_{L_{max}}$ as a function of $(d\alpha/dt)_e$ for a Mach Number of 0.400. These interpolated test points, which are independent of Mach number effects, are shown as the square test symbols in figure 7.

COMPARISON OF WIND-TUNNEL AND FLIGHT RESULTS

The comparison of the flight and wind-tunnel data on a pitching-velocity-effect basis given in figure 7 for $M = 0.400$ shows a similar variation of $C_{L_{max}}$ with rate of change of angle of attack. The indicated increases of $C_{L_{max}}$ are substantially of the same magnitude.

The flight pull-ups were made at rates of change of angle of attack as high as could ordinarily be obtained with this airplane. Although the model data presented extend to the same upper limit of $d\alpha/dt$ as the flight values, the model pitching velocities can be extended to higher values.

The comparison of the flight and wind-tunnel data on a maximum-lift-coefficient basis given in figure 8 shows a fair quantitative agreement and a similar decrease in maximum lift coefficient with increase in Mach number. The model values of $C_{L_{max}}$ shown in figure 8 were interpolated from figure 7 at the equivalent flight values of $d\alpha/dt$ and for the flight Mach numbers. All the values, with the corresponding Reynolds numbers, are listed in table I. Differences between corresponding airplane and model values of $C_{L_{max}}$ are also tabulated under the column heading $\Delta C_{L_{max}}$. The vertical scatter of the flight test points in figure 8 shows the magnitude of the variations due to pitching-velocity effect which were used in obtaining the interpolated flight test points shown in figure 7.

The fact that lower values of $C_{L_{max}}$ were obtained for the model than for the test airplane cannot be attributed to any one factor. Qualitatively it appears that the dissimilarities known to exist in power condition, Reynolds number, and fuselage configuration would tend to increase the flight values of $C_{L_{max}}$ with respect to the model values. It is also likely that indeterminable dissimilarities existed between the test airplane and its model, particularly in regard to the airfoil nose radius, on which the maximum lift coefficient depends to a marked degree.

CONCLUSIONS

The agreement obtained between the wind-tunnel results for a $\frac{1}{20}$-scale model of a conventional single-engine fighter airplane and flight results for the full-scale airplane indicates that the pitching-model technique should yield results applicable in the prediction of full-scale flight loads.

Results of the model tests show that the manner and rate of increase of maximum lift coefficient with rate of change of angle of attack vary with Mach number, with the trend at the low Mach numbers indicating that a limit of increase may have been reached.

Langley Aeronautical Laboratory
National Advisory Committee for Aeronautics
Langley Field, Va., July 30, 1948

REFERENCES

1. Rhode, Richard V.: Correlation of Flight Data on Limit Pressure Coefficients and Their Relation to High-Speed Burbling and Critical Tail Loads. NACA ACR No. L4I27, 1944.

2. Hamilton, William T., and Boddy, Lee E.: High-Speed Wind-Tunnel Tests of a 0.3-Scale Model of the P-47D Airplane. NACA ACR No. 5D20, 1945.

3. Furlong, G. Chester, and Fitzpatrick, James E.: Effects of Mach Number and Reynolds Number on the Maximum Lift Coefficient of a Wing of NACA 230-Series Airfoil Sections. NACA TN No. 1299, 1947.

TABLE I.- COMPARISON OF MAXIMUM LIFT COEFFICIENTS AND REYNOLDS NUMBERS OF TEST AIRPLANE AND PITCHING MODEL AT EQUIVALENT PITCHING RATES

Mach number	$C_{L_{max}}$		$\Delta C_{L_{max}}$	$d\alpha/dt$ (radians/sec)	$(d\alpha/dt)_o$ (radians/sec)	Reynolds number	
	Airplane	Model				Airplane	Model
0.269	1.64	1.57	0.07	0.458	9.80	9.05×10^6	0.620×10^6
.269	1.70	1.58	.12	.476	10.14	9.05	.620
.316	1.58	1.49	.09	.467	9.91	10.62	.718
.316	1.61	1.50	.11	.479	10.20	10.62	.718
.336	1.49	1.40	.09	.379	8.43	8.19	.758
.336	1.55	1.43	.12	.413	9.20	8.19	.758
.358	1.53	1.42	.11	.489	10.42	12.00	.801
.360	1.53	1.44	.09	.537	11.35	12.10	.803
.384	1.51	1.35	.16	.461	9.81	12.90	.850
.385	1.45	1.32	.13	.388	8.61	9.37	.851
.388	1.42	1.30	.12	.363	8.07	9.48	.858
.394	1.48	1.32	.16	.443	9.44	13.20	.868
.410	1.43	1.30	.13	.488	10.37	13.80	.896
.415	1.48	1.33	.15	.595	12.75	11.65	.905
.415	1.52	1.34	.18	.616	13.25	11.78	.905
.417	1.39	1.27	.12	.442	9.40	14.17	.908
.418	1.50	1.33	.17	.618	13.24	11.85	.910
.421	1.48	1.33	.15	.627	13.41	11.80	.915
.424	1.41	1.26	.15	.463	9.85	14.32	.920
.439	1.32	1.20	.12	.364	8.10	10.72	.947
.450	1.31	1.17	.14	.369	8.22	10.50	.965
.450	1.40	1.19	.21	.419	9.21	10.48	.965
.454	1.30	1.14	.16	.306	6.72	10.58	.970
.480	1.21	1.11	.10	.377	8.39	11.50	1.010
.485	1.22	1.10	.12	.382	8.52	11.48	1.018
.516	1.12	1.02	.10	.353	7.85	12.00	1.061
.520	1.12	1.03	.09	.380	8.48	12.53	1.068
.540	1.07	.97	.10	.362	8.06	12.60	1.092
.560	.97	.84	.13	.230	4.85	8.25	1.117

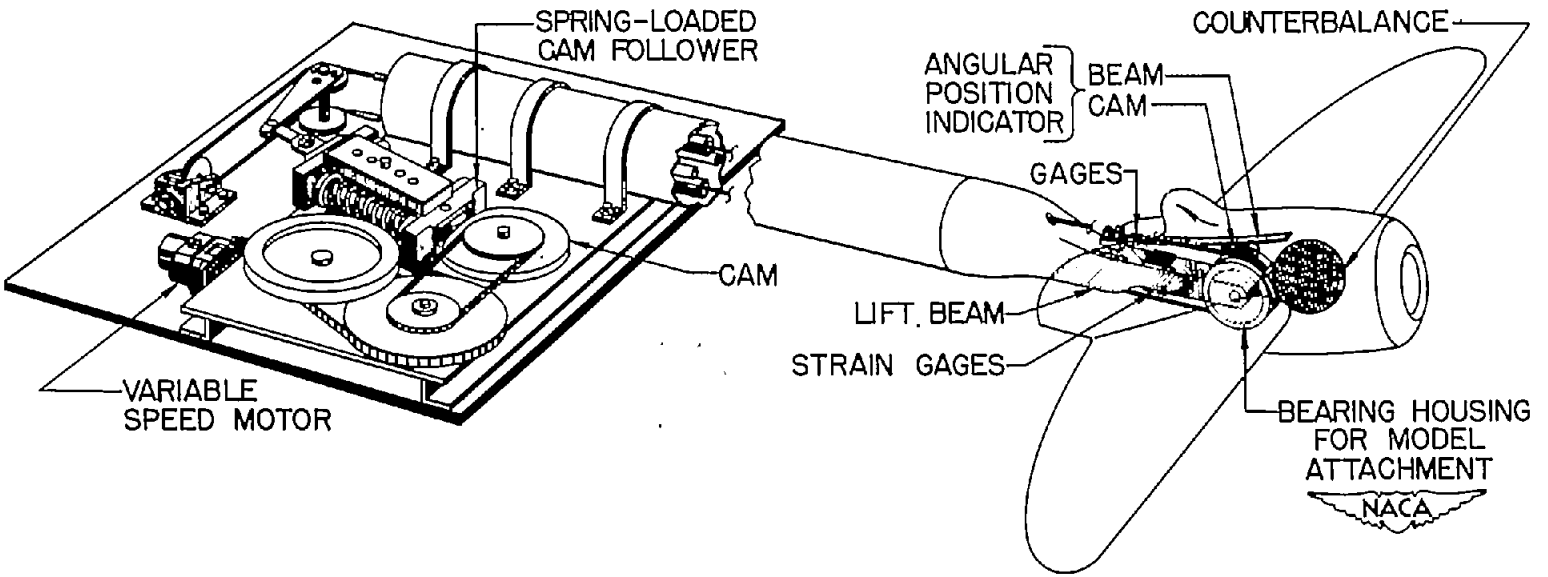

Figure 1.- Diagrammatic sketch of pitching-model apparatus.

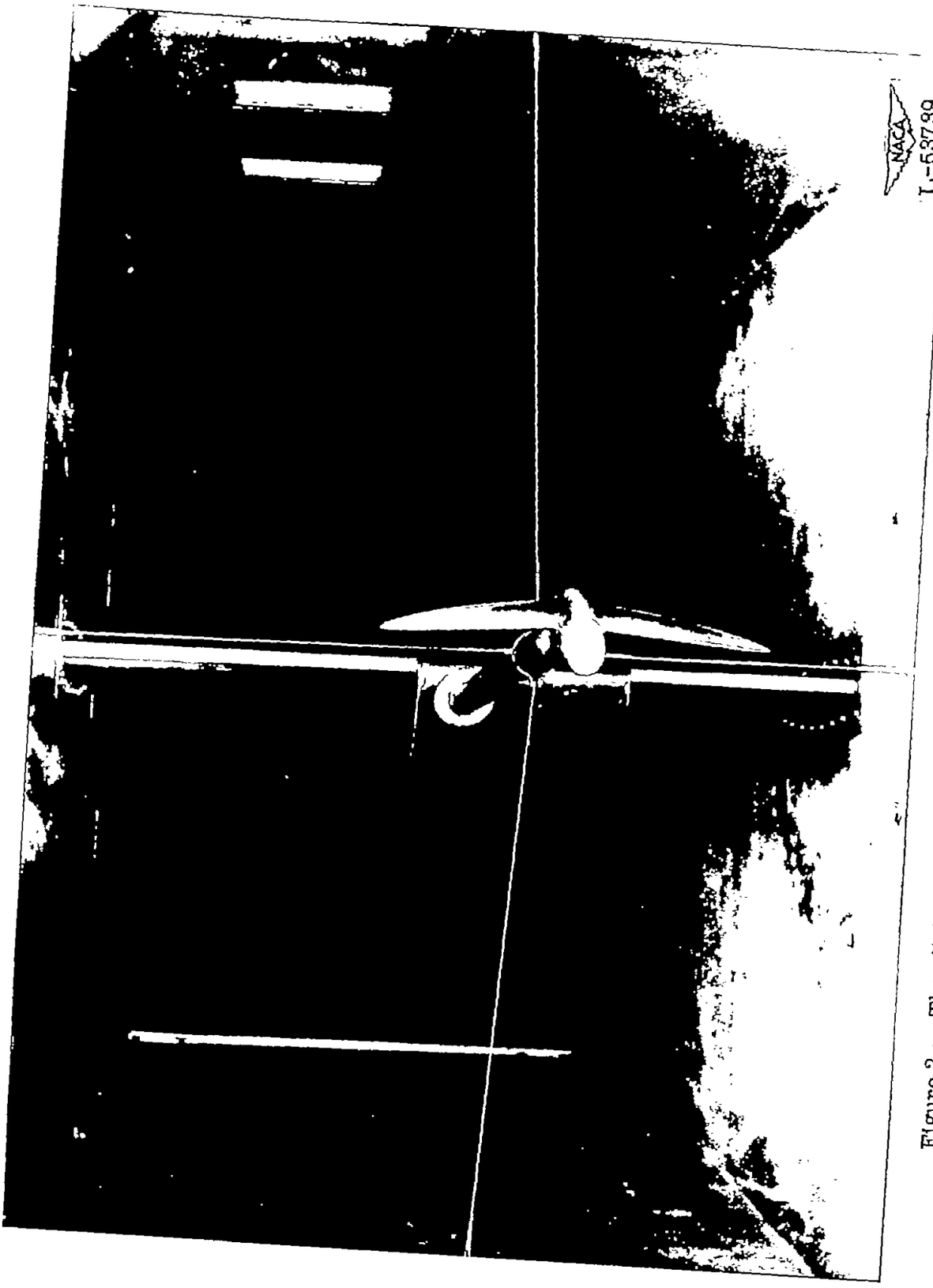

Figure 2.- The pitching model mounted in the Langley 7- by 10-foot high-speed tunnel.

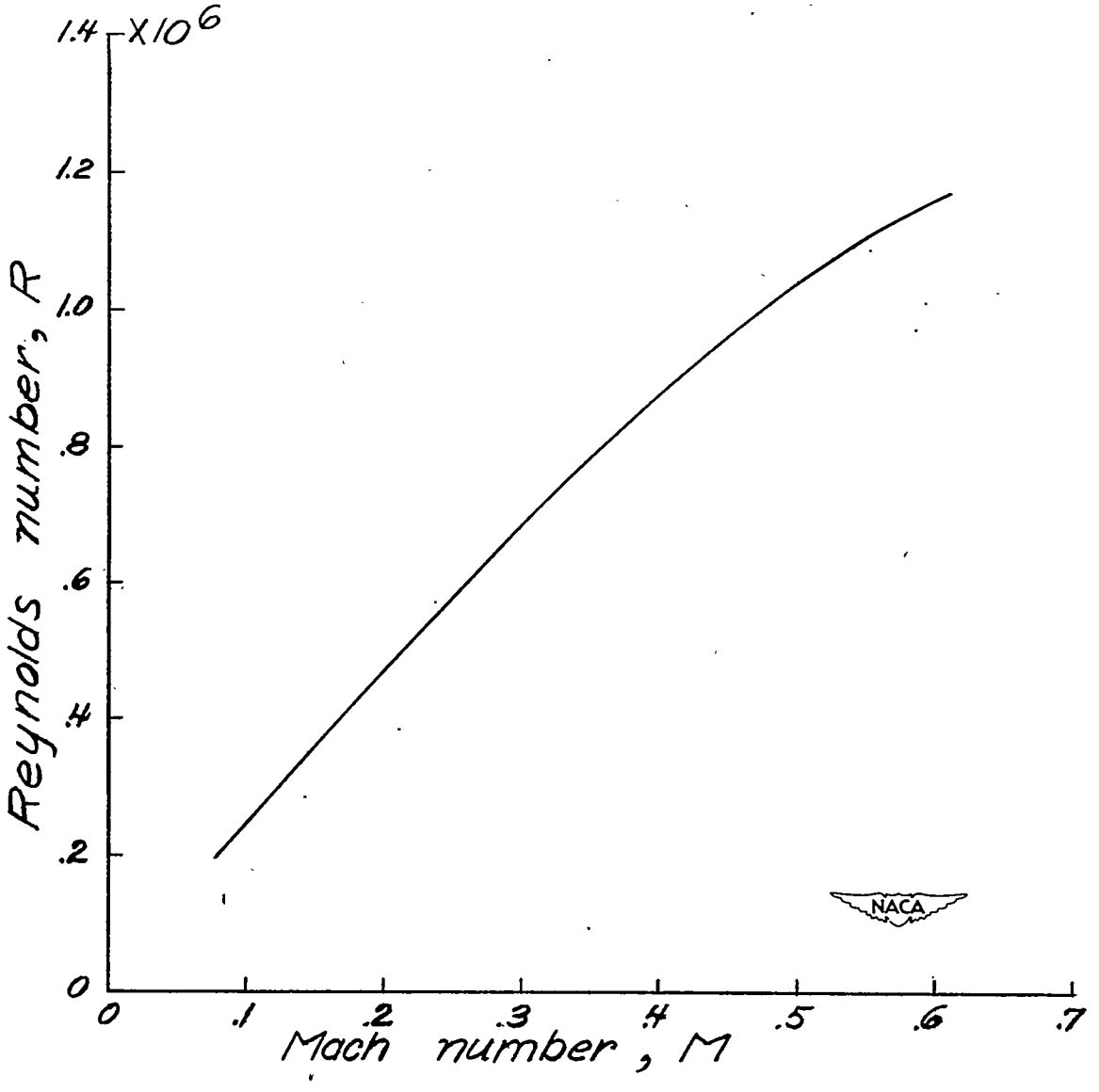

Figure 3.- Variation of Reynolds number with Mach number for the pitching-model tests.

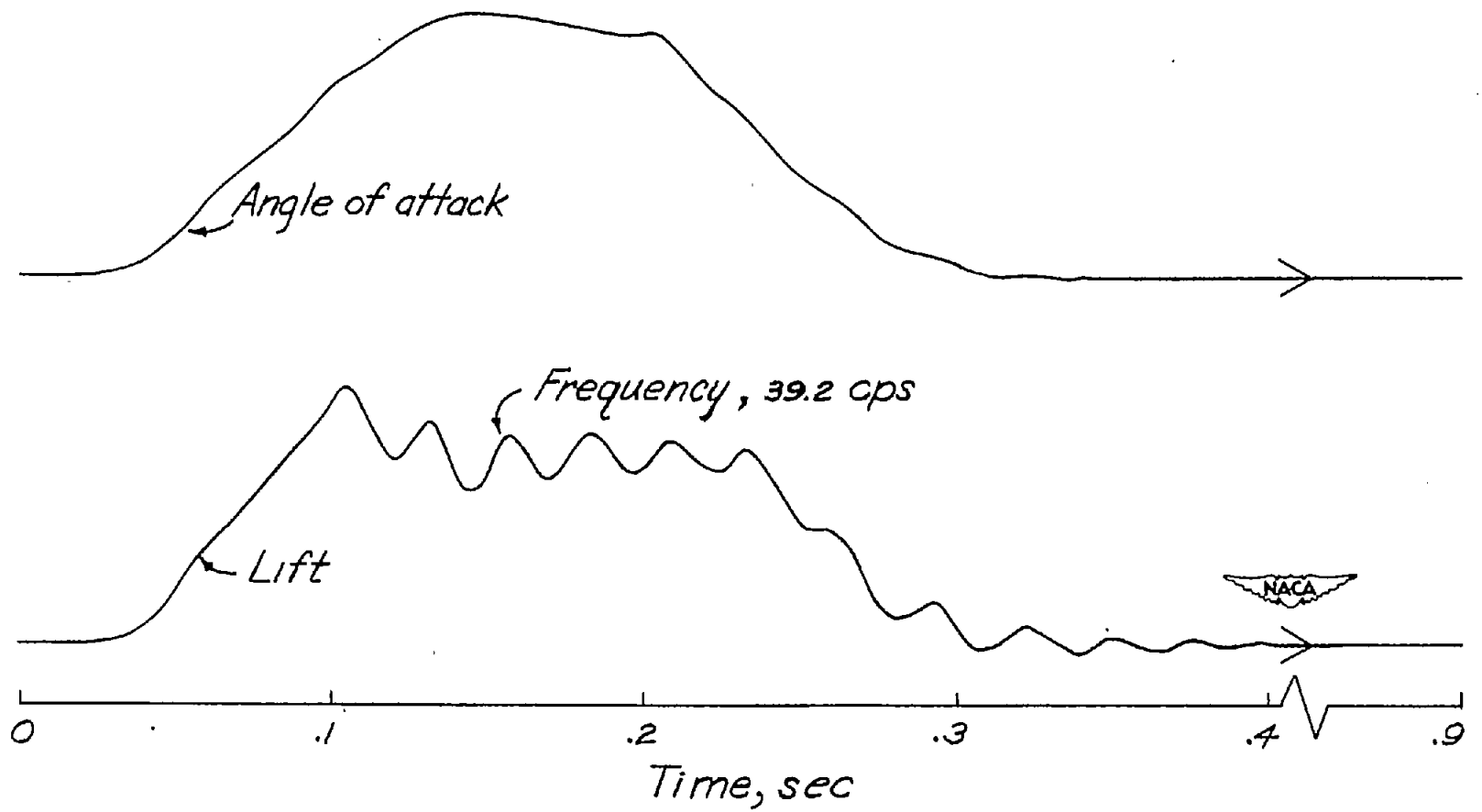

Figure 4.- Reproduction of a typical pitching-model record during one complete cam cycle for a Mach number of 0.400 and a pitching velocity of 5.75 radians per second.

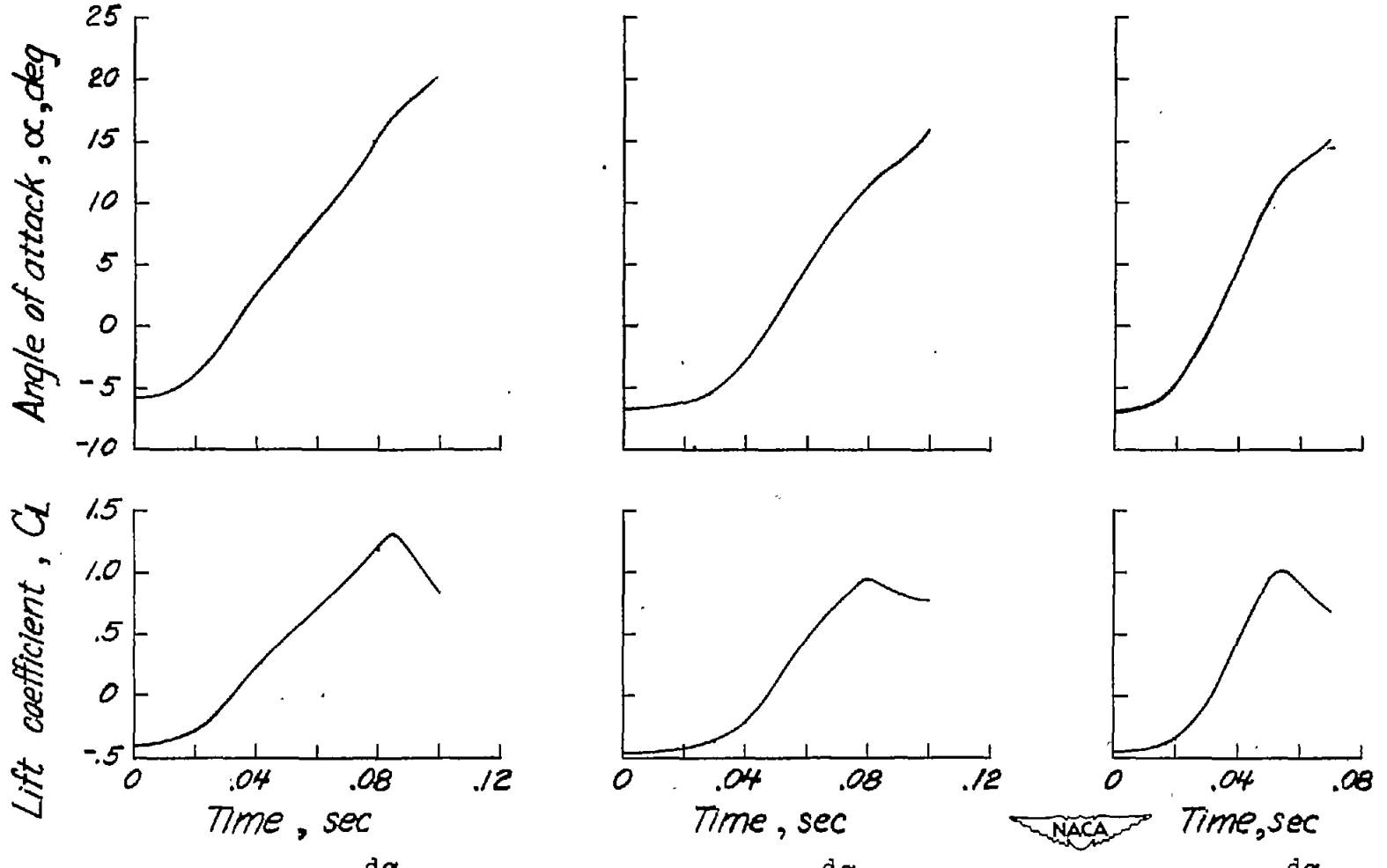

(a) M = 0.400; $\frac{d\alpha}{dt}$ = 5.75. (b) M = 0.542; $\frac{d\alpha}{dt}$ = 6.10. (c) M = 0.542; $\frac{d\alpha}{dt}$ = 8.72.

Figure 5.- Typical time histories of lift coefficient and angle of attack for the pitching model.

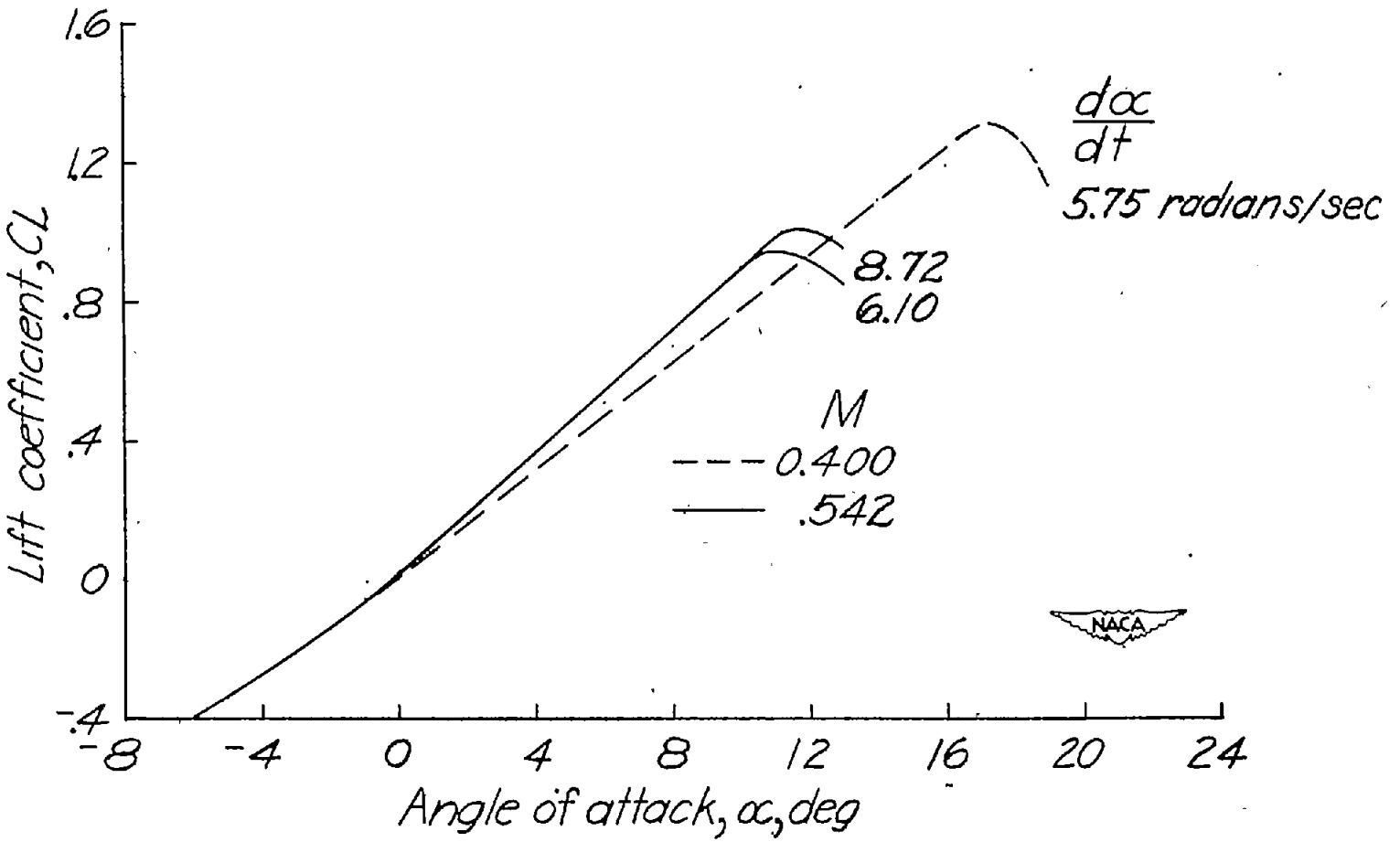

Figure 6.- Variation of lift coefficient with angle of attack for the typical time histories shown in figure 5 for the pitching model.

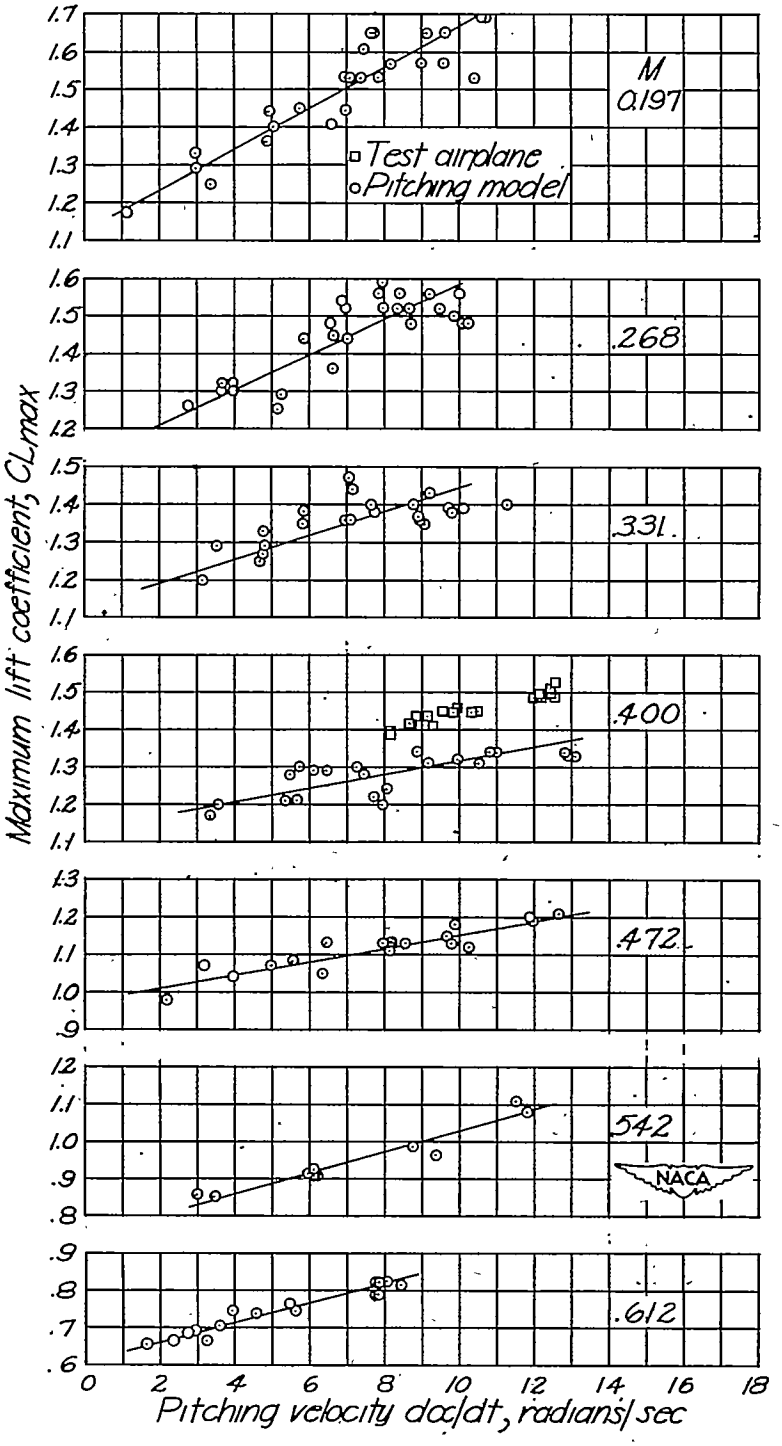

Figure 7.- Variation of maximum lift coefficient with rate of change of angle of attack for pitching model at various Mach numbers and comparison with similar results for test airplane at a Mach number of 0.400.

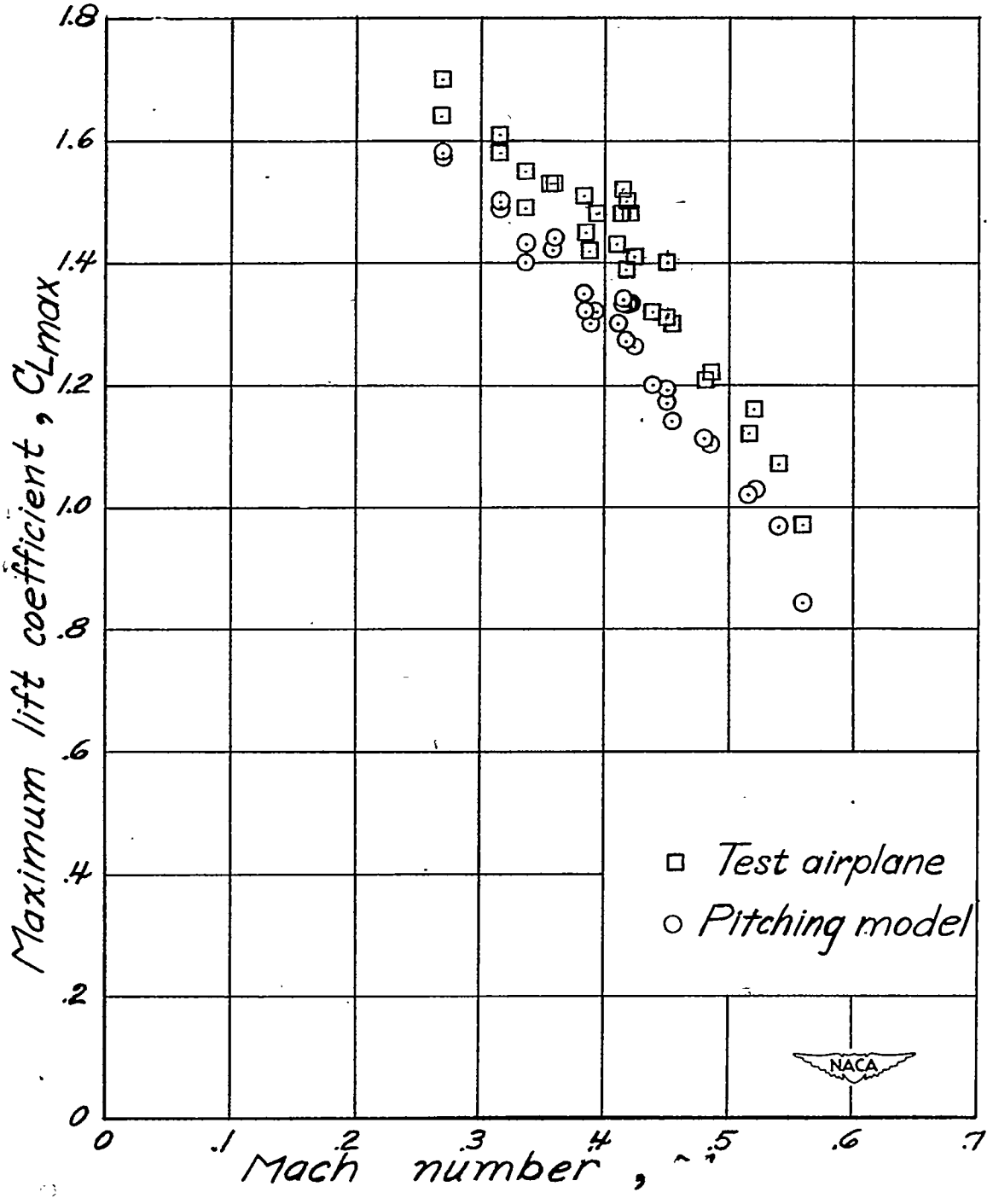

Figure 8.- Comparison of test airplane maximum lift coefficients corrected for tail load with those of the pitching model for corresponding Mach numbers and equivalent pitching rates.